ADAPTIVE DCT-BASED 1-D FILTERING OF POISSON AND MIXED POISSON AND IMPULSIVE NOISE

Vladimir V. Lukin[1], Dmitry V. Fevralev[1], Sergey K. Abramov[1], Sari Peltonen[2], Jaakko Astola[2]

[1] Department of Transmitters, Receivers and Signal Processing, National Aerospace University, Chkalova Str. 17, 61070 Kharkov, Ukraine, Telephone/Fax: +38 (057) 3151186, E-mails: lukin@xai.kharkov.ua, fevralev@mail.ru, ask379@mail.ru

[2] Tampere University of Technology, Department of Signal Processing, P. O. Box 553, FIN-33101, Tampere, Finland, Telephone: +358 3 3115 2923, Fax: +358 3 3115 3857, E-mails: sari.peltonen@tut.fi, jaakko.astola@tut.fi

ABSTRACT

Practical cases where a 1-D signal is corrupted by mixed Poisson and specific impulsive noise are considered. The requirements to the filtering method are discussed. It is shown that DCT based filters combined in adaptive manner with some robust filter, e.g., a standard median filter, can effectively be applied for noise removal in the considered case. Different modifications of the DCT based filter are analyzed. It is demonstrated that the DCT based filter can either be applied together with a pair of Anscombe pointwise transforms or in a "signal-dependent" manner without such transforms. It is shown via numerical simulations that the latter way may be preferable.

1. INTRODUCTION

Poisson distribution often describes the statistical characteristics of processes and noise met in the practice [1-6]. In particular, this frequently holds when some discrete measuring system collects temporal data for which the estimate (sample) obtained for each elementary interval of fixed duration corresponds to the count of some events, for example, the number of registered particles [2, 3]. The Poisson noise can also be observed in the X-ray medical and tomographic data [4-7].

Commonly 1-D Poisson type signals, being the outputs of radiation sensors, vary rather slowly and their values are smaller than 10. A typical fragment is demonstrated in Fig. 1.

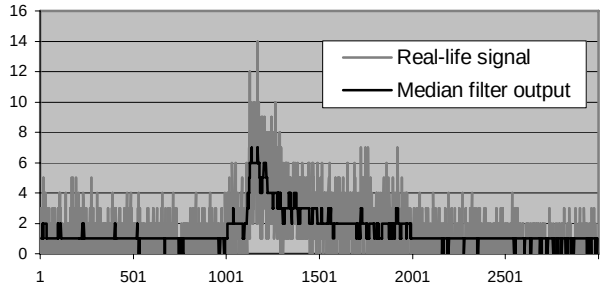

Fig. 1. A real life slowly varying fragment of the radiation sensor signal

One more peculiar feature of the considered 1-D signals is the possible presence of specific impulsive noise. This impulsive noise can also be treated as abnormal measurements (estimates). There are various reasons for the occurrence of such impulsive noise. One of them can be the external interferences that influence the sensors. At the same time, "information impulses" can be present as well. The difference between the "information impulses" and the aforementioned abnormal measurements is in their duration (widths). Specialists are able to establish in advance the duration of the impulses (characterized by some number of samples N_{inf}) that can be considered as information whilst the other ones with $N_{abn} < N_{\text{inf}}$ relate to the impulsive noise to be removed. An example of the real life signal that contains two "information impulses" (in the right part) and two abnormal measurements (of smaller amplitudes and with smaller indices of the corresponding samples) is represented in Fig. 2.

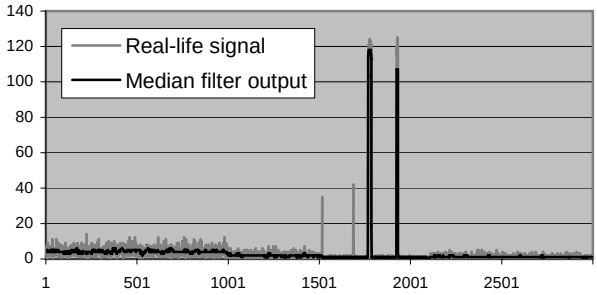

Fig. 2. An example of the signal that contains two "information impulses" and two abnormal measurements

Clearly such data are to be processed (filtered) [2, 3, 8] in order to solve three tasks: a) to reduce the oscillations due to fluctuative noise with Poisson probability density function (PDF); b) to remove the abnormal measurements (outliers, impulsive noise); and c) to preserve the useful information including the "information impulses".

There are many different ways to process 1-D signals with the properties (features) described above. The simplest way is to apply the standard median filter (SMF). Its output for the scanning window size $N_{med} = 15$ is shown in Figures 1 and 2 by the black lines. The SMF easily solves the tasks of preservation of the "information impulses" and rejection of impulsive noise. It also partly suppresses fluctuative noise.

However, the degree of its suppression is not enough [3]. More efficient reduction is required, especially in the "background" fragments of the signals where they vary slowly and have relatively small values. One solution is to apply adaptive nonlinear filters [3]. But this is not the only solution. Recently several transform based approaches to filtering the data corrupted by the Poisson noise have been proposed [4, 7]. In this case, two ways to follow are possible. The first one is to apply the three-stage procedure $H(.) \to F(.) \to H^{-1}(.)$ where $H(.)$ and $H^{-1}(.)$ denote a pair of direct and inverse pointwise transforms, respectively; $F(.)$ denotes a filter. A pointwise transform widely used in the processing of signals and images corrupted by the Poisson noise is Anscombe transform [9]. When the direct transform is applied, the signal-dependent Poisson noise converts to additive noise with practically constant variance equal to 0.25 for $\lambda(i)>3$ where $\lambda(i)$ denotes the true signal value in the i-th sample of the 1-D signal. Additive character of the noise simplifies application of the transform based denoising techniques, both wavelet and DCT based [4, 10]. However, 1-D DCT based filtering has not yet been studied in combination with the Anscombe transform.

In turn, there also are DCT based methods for the filtering of data that are corrupted by signal dependent noise [10] but they have not been modified and tested for the Poisson noise removal. These methods do not require use of any pointwise transform since they exploit locally adapting threshold value by taking into account a priori known dependence of the local variance on the local mean. For the Poisson PDF such dependence is a priori known and fixed: the local variance is equal to the local mean. However, there are several ways to exploit this dependence. Besides, the transform (wavelet and DCT) based denoising techniques are, in general, unable to remove the impulsive noise.

Therefore, this paper has two main goals. The first goal is to analyze the efficiency of the DCT based methods when they are applied to the filtering of 1-D signals corrupted by the Poisson noise. The second goal is to design special methods that are able to perform well enough for the removal of the mixed Poisson and impulsive noise.

2. NOISE MODEL

In this paper, we consider a model of a 1-D signal $S(t_i) = S(i), \quad i = 1,...,I$, where I denotes the number of our signal samples. We assume that at each i-th moment of time $S(i)$ obeys the Poisson distribution

$$f(i,k) = \frac{e^{-\lambda(i)}\lambda(i)^k}{k!}, k = 0,...,\infty, \qquad (1)$$

where $\lambda(i)$ is the true value, $\lambda \geq 0$. Note that the values of $S(i)$ can differ a lot from $\lambda(i)$ since the mean m_P and the variance σ_P^2 are both equal to λ and $\sigma_P = \sqrt{\lambda}$.

The model (1) corresponds to the case of impulsive noise absence. However, as it has been said earlier, some samples of the signal can be corrupted by the impulsive noise. One can consider a sample value to be impulsive noise (an outlier) if, e.g., $S(i)$ differs from the corresponding $\lambda(i)$ by more than $5\sigma_P$. Then, the model for the observed 1-D process could be the following

$$S(i) = \begin{cases} S_n(i), & \text{with probability } 1-p \\ \lambda(i) + A(i), & \text{with probability } p \end{cases} \qquad (2)$$

where $S_n(i)$ defines a "pure" Poisson process with statistics determined by (1), $A(i)$ corresponds to the outliers with aforementioned properties, and p denotes the probability of the impulsive noise occurrence. This model takes into account the property of the real life abnormal measurements that the impulsive noise is positive, i.e., the values for the samples corrupted by outliers are considerably larger than the corresponding true values $\lambda(i)$.

One should keep in mind that even if p=0, the accuracy of the primary estimate is characterized by the relative error $\sigma_P / m_P = 1/\sqrt{\lambda}$. This means that for the small $\lambda(i)$ the accuracy is low. But in many practical situations (see the real life signal plots in Figures 1 and 2), radiation sensors operate in the so-called background estimation mode for which $\lambda(i)$ is smaller than 10. This confirms the necessity to carry out filtering of such signals in order to provide better accuracy of the radiation parameter estimation and to avoid false alarms in the detection of emergency situations by the control systems.

An example of the test signal corrupted by the mixed noise (2) is presented in Fig. 3. This test signal has been also used in [3]. It models the practical situations of the background mode, sharp changes of $\lambda(i)$ (indices 3200 and 4700), and slowly varying signal (the fragment from the 7100-th sample to the end of the signal). It also contains one "information impulse" in the neighbourhood of the 2500-th sample.

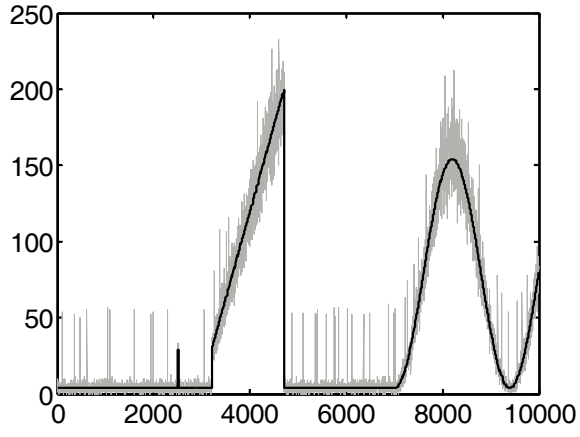

Fig. 3. A true test signal and the signal corrupted by mixed Poisson and impulsive noise (gray line)

3. DCT-BASED FILTERING WITH ANSCOMBE TRANSFORMS

There are several variants of the Anscombe transform described in the literature. The most commonly used one is [9, 11]

$$S_H(i) = S_{D\,Ans}(i) = [S(i) + 3/8]^{1/2}. \quad (3)$$

The PDF of the data obtained after the direct Anscombe transform (3) (in the case of constant $\lambda(i)$) occurs to be rather close to the discrete Gaussian with the mean equal to $(\lambda + 1/8)^{1/2}$. For λ=6, this PDF and its approximation by the Gaussian PDF with the mean $\sqrt{6.125}$ and the variance σ^2_{At}=0.25 are shown in Fig. 4.

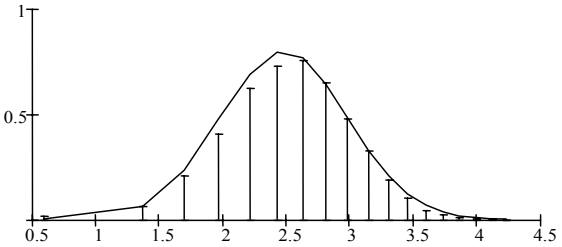

Fig. 4. The histogram of the Poisson 1-D process with λ=6 after direct the Anscombe transform (3) and its approximation

The dependence of σ^2_{At} on λ is given in Fig. 5. As seen, for λ>3 the variance σ^2_{At} is practically constant and equal to 0.25. For smaller λ, the variance σ^2_{At} is slightly smaller than 0.25. This creates favorable conditions for applying transform based filtering to the signal $\{S_H(i), i = 1,..., I\}$.

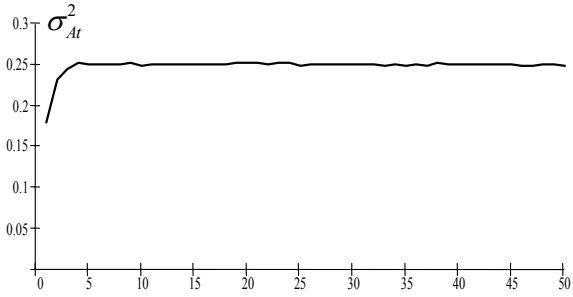

Fig. 5. Dependence of σ^2_{At} on λ after the direct Anscombe transform (3)

The conventional DCT based filtering is performed in three steps [13]. First, for each block (window) of fixed size N_{bl}, the direct DCT is carried out. At the second step, thresholding of the obtained DCT coefficients is performed. Third, inverse DCT is applied to the set of thresholded DCT coefficients.

At step 2, either hard or soft thresholding can be used where the threshold is commonly set as $T = \beta\sigma$ where β is a factor and σ denotes the standard deviation of the additive noise. After the inverse DCT, the output (filtered) values are obtained for the entire block. Moreover, the blocks can be non-overlapping, partly overlapping, or minimal shift overlapping (spatially invariant). In the latter two cases, the obtained filtered values are to be averaged for each sample.

The performance of DCT based denoising described above depends upon several parameters of the algorithm, namely, the block size, the threshold value defined by β and the thresholding type (hard, soft, etc.), and the block overlapping. Also, the performance depends upon the processed signal. Below we have analyzed hard thresholding (commonly, filtering with hard thresholding preserves details better [12]). The considered block size was equal to different powers of two to provide the algorithm computational efficiency [12].

There are also several variants of the inverse Anscombe transform. We tested some of them and finally decided to apply the inverse Anscombe transform that is defined as $Y_{out}(i) = (S^{out}_H(i))^2 - 1/8$ where $S^{out}_H(i)$ is the i-th sample of the filtered signal $\{S^{out}_H(i), i = 1,..., I\}$. In fact, this is not exact inverse of the forward transform, but it produces almost unbiased output for the signal fragments where $\lambda(i) = Const$.

To characterize the efficiency of the filtering, let us consider several quantitative parameters. First, we analyze the conventional MSE. However, it does not adequately characterize the reachable accuracy of the signal estimation. It is often desirable to analyze the relative accuracy of the signal estimation for each sample. For this purpose, it is reasonable to analyze a relative error function $\Delta S(i) = (S_f(i) - \lambda(i))/\lambda(i)$ and its statistical properties. For example, it can be required that one has to minimize the number of samples for which $|\Delta S(i)| > 0.2$ [3]. Then a reasonable quantitative criterion is the probability P_{exc} of the event $|\Delta S(i)| > 0.2$.

Table 1. Performance of DCT based filter

N_{bl}	Overlapping	β	MSE	P_{exc}
16	Full (spatial invariant)	2.5	3.19	0.076
		3	2.18	0.044
		3.5	2.02	0.036
		4	2.07	0.034
		4.5	2.19	0.033
	N_{bl}/2 shift	3.5	2.47	0.047
	Without Overlapping	3.5	3.17	0.075
32	Full (spatial invariant)	2.5	2.53	0.048
		3	1.66	0.015
		3.5	**1.59**	0.01
		4	1.68	0.009
		4.5	1.87	0.009
	N_{bl}/2 shift	3.5	2.02	0.018
	Without Overlapping	3.5	2.71	0.029
64	Full (spatial invariant)	2.5	2.7	0.035
		3	2.08	0.011
		3.5	2.02	0.008
		4	2.18	**0.007**
		4.5	2.31	0.007
	N_{bl}/2 shift	3.5	2.62	0.016
	Without overlapping	3.5	4.86	0.028

Let us now consider numerical simulation results obtained for the test signal presented in Fig. 3 for the case p=0. They are presented in Table 1. There and below the values of the MSE and P_{exc} are obtained from 100 realizations (the MSE for the original signal is about 40). The analysis of these data shows the following.

First, in practically all cases, the smallest values of MSE and P_{exc} are provided for β=3.5 or 4. Thus, for processing with the shift N_{bl} /2 and without overlapping we present the obtained results only for β=3.5.

Second, as can be expected, the smallest values of MSE and P_{exc} are observed for the DCT based filtering with full overlapping. Note that this method requires a considerably larger amount of computations than for the two other algorithms of denoising. An example of the output signal is demonstrated in Fig. 6. The plot of $\{\Delta S(i)\}$ is presented in Fig. 7. As seen, the requirement $|\Delta S(i)| < 0.2$ is provided for almost all samples except those ones in the neighbourhood of the sharp transitions of the test signal.

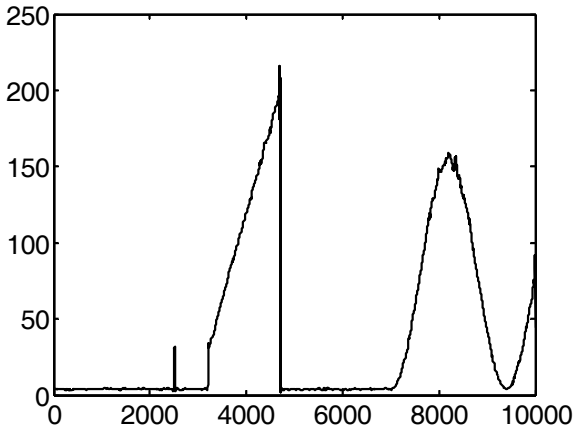

Fig. 6. Output of the three-stage procedure for the DCT filter with full overlapping, N_{bl}=32, β=3.5

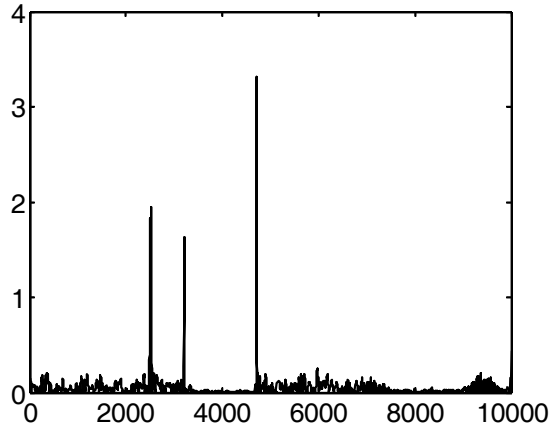

Fig. 7. $\{\Delta S(i)\}$ for the output signal in Fig. 6

4. ADAPTIVE DCT-BASED FILTERING

Consider now the DCT-based filtering without the pointwise (Anscombe) transform of the data. The possibility to locally adapt the parameters of the DCT-based filtering [7, 10] is one of the main advantages of this approach. Such parameters can be the block size and/or shape [7] and the threshold value [10]. The basic rule for filtering signal dependent noise (Poisson, pure multplicative, film-grain, etc.) is to locally set th threshold in a block using a priori known or pre-estimated relation between the local variance and the local mean [7, 10, 12]. For the Poisson noise, such dependence is known a priori. For the constant signal fragments, the local variance is approximately equal to the local mean.

In general, the adaptive DCT based filtering presumes setting an individual threshold for each block

$$T_{bl} = \beta \hat{\sigma}_{bl} \tag{4}$$

where $\hat{\sigma}_{bl}$ denotes an estimate of the standard deviation of the noise for a given block. If there is a known relation between the local standard deviation and the local mean $\sigma_{loc} = f(\bar{I})$, then it is possible to set the threshold for each block as

$$T_{bl} = \beta(f(\hat{\bar{I}}_{bl})), \tag{5}$$

where $\hat{\bar{I}}_{bl}$ is some estimate of the mean in the block. Both conventional and robust estimates can be used.

Table 2. Performance of the adaptive DCT based filter that uses $\hat{I}_{bl}^{mean}$

N_{bl}	Overlapping	β	MSE	P_{exc}
16	Full (spatial invariant)	2.5	3.13	0.073
		3	2.2	0.042
		3.5	2.1	0.034
		4	2.1	0.033
		4.5	2.21	0.033
	N_{bl} /2 shift	3.5	2.47	0.046
	Without Overlapping	3.5	3.22	0.074
32	Full (spatial invariant)	2.5	2.52	0.046
		3	1.64	0.015
		3.5	**1.53**	0.01
		4	1.59	0.009
		4.5	1.75	0.009
	N_{bl} /2 shift	3.5	1.78	0.018
	Without Overlapping	3.5	2.48	0.029
64	Full (spatial invariant)	2.5	2.6	0.035
		3	1.89	0.012
		3.5	1.8	0.009
		4	1.9	**0.009**
		4.5	2.04	0.009
	N_{bl} /2 shift	3.5	2.14	0.018
	Without Overlapping	3.5	4.55	0.024

For the Poisson noise one has $\sigma_{loc} = f(\bar{I}) = \sqrt{\bar{I}}$. Thus, for each block, we propose to obtain some estimate $\hat{\bar{I}}_{bl}$ and to calculate $T_{bl} = \beta\sqrt{\hat{\bar{I}}_{bl}}$. Below we consider two simplest vays to obtain $\hat{\bar{I}}_{bl}$ – to calculate it as the mean in a block ($\hat{I}_{bl}^{mean}$) or as the median value ($\hat{I}_{bl}^{med}$).

As follows from the analysis in the previous section, the performance of the described adaptive DCT based denoising has to depend upon the block size, how much they overlap, and the parameter β. Therefore, we have obtained numerical simulation data for the same test signal with different sets of the filter parameters. They are presented in Tables 2 and 3 for the cases of using the estimates $\hat{I}_{bl}^{mean}$ and $\hat{I}_{bl}^{med}$, respectively.

It is seen by analyzing the data in Tables 2 and 3 that the main tendencies observed for the data in Table 1 remain the same. Again, the block overlapping produces the best results. The best value of β is equal to 3.5 or 4.0, and the best block size is 32. For the same β, N_{bl} and overlapping, the values of MSE and P_{exc} in Table 2 are practically the same (or even slightly worse) than in Table 1. At the same time, the values of MSE and P_{exc} given in Table 3 are considerably better than the corresponding values in Tables 1 and 2 (for convenience of comparison, the smallest values of MSE are marked by bold in all tables).

Table 3. Performance of the adaptive DCT based filter that uses $\hat{I}_{bl}^{med}$

N_{bl}	Overlapping	β	MSE	P_{exc}
16	Full (spatial invariant)	2.5	3.65	0.085
		3	2.59	0.048
		3.5	2.31	0.037
		4	2.21	0.033
		4.5	2.21	0.033
	N_{bl} /2 shift	3.5	2.73	0.049
	Without Overlapping	3.5	4.63	0.078
32	Full (spatial invariant)	2.5	2.5	0.055
		3	1.56	0.02
		3.5	**1.37**	0.011
		4	1.39	**0.009**
		4.5	1.41	0.009
	N_{bl} /2 shift	3.5	1.82	0.022
	Without Overlapping	3.5	2.43	0.032
64	Full (spatial invariant)	2.5	2.48	0.045
		3	1.66	0.016
		3.5	1.48	0.012
		4	1.47	0.011
		4.5	1.42	0.01
	N_{bl} /2 shift	3.5	2.2	0.022
	Without overlapping	3.5	5.02	0.031

We have analyzed why the adaptive DCT based filter which exploits estimates $\hat{I}_{bl}^{med}$ performs better than the other DCT based filters. For this purpose, we have calculated local MSE values in the neighborhoods of the information impulse (MSE_{ii}), the first sharp transition (MSE_{re1}) and the second sharp transition (MSE_{re2}).

The sizes of the intervals for which these local MSE values have been evaluated are 82, 64, and 64 samples, respectively. The parameters of the DCT filters were close to optimal: block size was 32 with full overlapping and β=3.5. The simulation data are given in the first two rows of Table 4.

Table 4. Local MSE for different filters

Filtering technique	MSE_{ii}	MSE_{re1}	MSE_{re2}
DCT with Anscombe transforms	8.00	7.15	85.99
Adaptive DCT using $\hat{I}_{bl}^{med}$	6.32	5.56	57.27
Adaptive DCT using $\hat{I}_{bl}^{mean}$	7.31	6.59	77.61
With post-processing by the median filter, $N_{med} = 15$	5.74	4.94	47.30

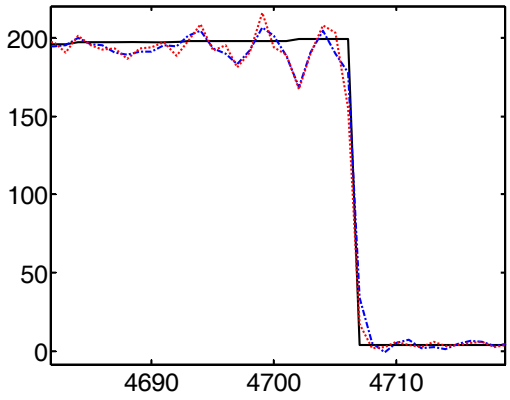

Fig. 8. A fragment of one realization of outputs for the adaptive DCT filter with $\hat{I}_{bl}^{med}$ (dashed line) and three-stage filtering (dotted line). True (noise-free) signal is shown by solid (black) line

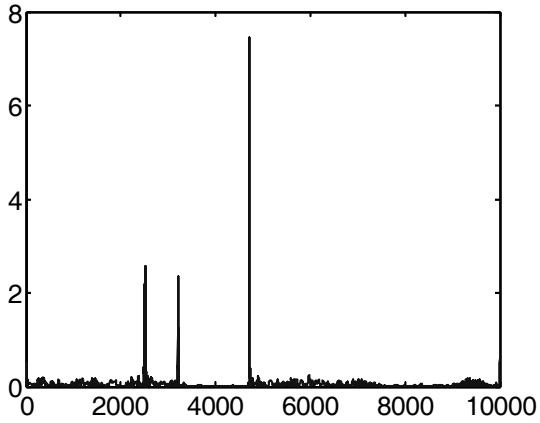

Fig. 9. $\{\Delta S(i)\}$ for the adaptive DCT based filtering that uses $\hat{I}_{bl}^{med}$

As seen, the local MSE values for the three-stage DCT-based filtering with the Anscombe transforms are considerably worse (larger) than for the adaptive DCT based filtering using $\hat{I}_{bl}^{med}$. Distortions are especially larger in the neighborhoods of sharp high contrast transitions (see Fig. 8). Fig. 9 presents the relative error $\{\Delta S(i)\}$ for the adaptive DCT based filter that uses $\hat{I}_{bl}^{med}$ (full overlapping, $\beta \approx 3.5$, N_{bl}=64).

The three considered versions of the DCT based filters have also been analyzed for another test signal (solid line) presented in Fig. 10. This test signal has been obtained of the known signal Heavisine [13] by stretching (to 8192 samples), adding a constant (to make the test signal non-negative), and rounding-off (to the closest integer). Then, realizations of the Poisson noise have been generated. One of the noisy signals is shown in Fig. 10 by grey.

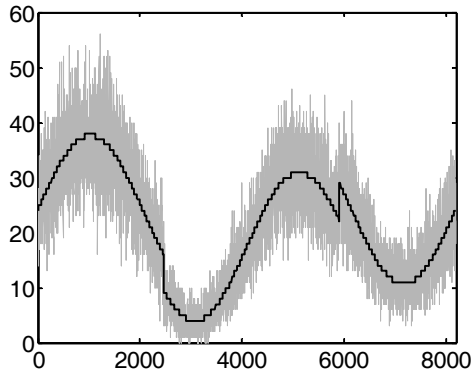

Fig. 10. The second test signal (solid black line) and its noisy realization (grey line)

The simulation data obtained for 100 realizations of noise are presented in Table 5 (input MSE=21). Below we consider only the case of full overlapping. As seen, for this test signal there is practically no difference in the values of the MSE and P_{exc} obtained for all three methods for a given set of filter parameters (N_{bl}, β). The optimal choice of β is about 4. However, for this test signal the best results (minimal MSE and minimal P_{exc}) have been obtained for N_{bl}=64. Recall, that for the first test signal (Fig. 3) the best results were observed for N_{bl}=32. The reason is that the second test signal (Fig.10) is smoother.

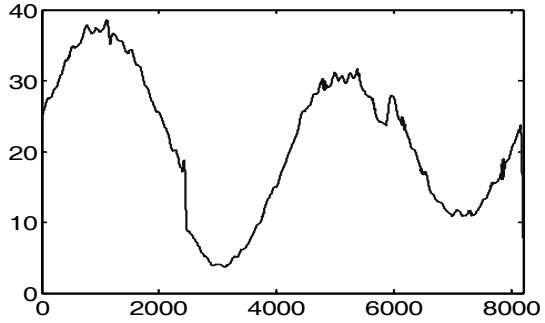

Fig. 11. The output of the DCT based filter that uses $\hat{I}_{bl}^{med}$ for the noisy test signal in Fig. 10

The output of the DCT based filter that uses $\hat{I}_{bl}^{med}$ for the second test signal is demonstrated in Fig. 11 (N_{bl}=64, β=4). As seen, good suppression of the noise is observed simultaneously with the preservation of the information features.

Joint analysis of simulation data for both test signals shows that the DCT based filtering method that uses $\hat{I}_{bl}^{med}$ provides benefits in comparison to other two techniques if a signal contains sharp transitions.

Table 5. Performance of DCT based filters for the test signal in Fig. 10

		DCT with Anscombe		DCT based on $\hat{I}_{bl}^{mean}$		DCT based on $\hat{I}_{bl}^{med}$	
N_{bl}	β	MSE	P_{exc}	MSE	P_{exc}	MSE	P_{exc}
16	2.5	1.58	0.019	1.55	0.018	1.60	0.020
	3	1.08	0.008	1.07	0.007	1.07	0.009
	3.5	0.95	0.006	0.96	0.006	0.96	0.006
	4	0.94	0.006	0.93	0.005	0.94	0.006
	4.5	0.94	0.005	0.93	0.005	0.94	0.006
32	2.5	1.10	0.011	1.08	0.010	1.11	0.013
	3	0.64	0.003	0.63	0.003	0.65	0.004
	3.5	0.53	0.002	0.54	0.002	0.53	0.003
	4	0.52	0.002	0.52	0.002	0.52	0.003
	4.5	0.52	0.002	0.51	0.002	0.52	0.003
64	2.5	0.88	0.007	0.87	0.007	0.90	0.010
	3	0.43	0.002	0.42	0.002	0.43	0.004
	3.5	0.34	0.002	0.35	0.002	0.34	0.003
	4	**0.33**	0.002	**0.32**	0.002	**0.33**	0.003
	4.5	**0.33**	0.002	0.33	0.002	0.33	0.003

5. ROBUST MODIFICATIONS OF DCT BASED FILTERS

Consider now the case of mixed noise. For this purpose, let us at the beginning artificially add only three impulses into the test signal corrupted by the Poisson noise. These impulses have been added in the 1000-th, 2000-th and 6000-th samples. All impulses had $A(i)$=50. The output of the adaptive DCT based filter that uses $\hat{I}_{bl}^{med}$ is presented in Fig. 12. As seen, the impulses practically remained "untouched". Moreover, the efficiency of the Poisson noise suppression in the neighbourhoods of the impulses became poorer than it was in the case of impulse absence.

As the result, the relative error in the neighborhoods of samples corrupted by impulses has radically increased (see Fig. 13 and compare with Fig. 8). In comparison to the case of p=0, the values σ_{out}^2 and P_{exc} have radically increased. The MSE has become equal to 1.90 and P_{exc} has reached 0.019, i.e., they have increased by more than

1.4 times. This example clearly shows that even a few impulses present in the observed 1-D signal considerably worsen the performance of the adaptive DCT based filter. The same takes place if the DCT based denoising is applied in combination with the Anscombe transforms. Thus, some special means to avoid this drawback of the DCT based filtering should be used.

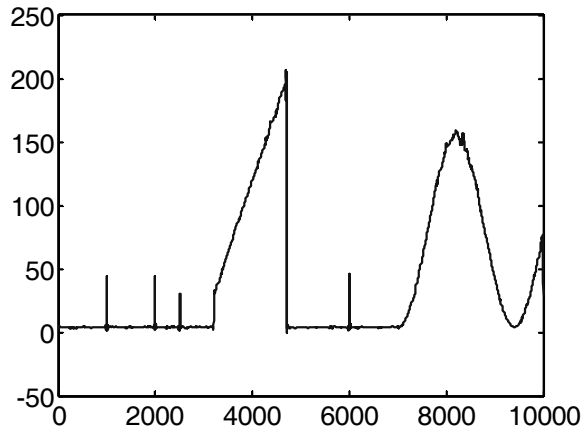

Fig. 12. Output signal for the adaptive DCT based filter that uses $\hat{I}_{bl}^{med}$ in case of impulsive noise presence

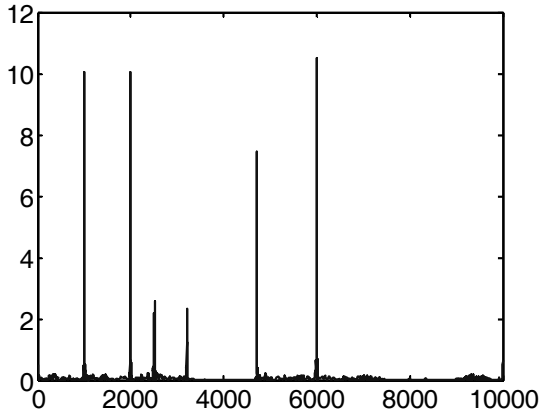

Fig. 13. $\{\Delta S(i)\}$ for the output signal in Fig. 12

One option is to apply a two-stage filtering similarly to the way it was proposed for the mixed noise removal in images [14]. At the first stage, the adaptive DCT based denoising is used, then the standard median filter is applied to its output. For the adaptive DCT based filter the full-overlapping processing is recommended. We used the block size 32, the estimate $\hat{I}_{bl}^{med}$ and $\beta \approx 3.5$ (since it provided the best results). For the standard median filter the recommended scanning window size is 15.

Consider first the results for the case of p=0. The obtained values are: σ_{out}^2=1.25, P_{exc}=0.008. They are smaller than for the best adaptive DCT based filter (see data in Table 3). The local MSE values for this two stage denoising are given in Table 4 (see the row "With post-processing by the median filter, $N_{med}=15$"). As seen, the local MSE values are slightly better than for the adaptive DCT based filter.

Let us now analyze the example of the presence of three impulses considered above. For this case, we have obtained σ_{out}^2=1.30, P_{exc}=0.009. This means that the influence of impulses has been greatly reduced.

Finally, consider the case of mixed noise with p=0.005. This noisy signal is shown in Fig. 3. After the first stage of processing, i.e., for the output of the adaptive DCT based filter we have obtained σ_{out}^2=8.11, P_{exc}=0.094. As seen, these values are several times larger than for the case of p=0. The output signal is given in Fig. 14. Almost all impulses are kept practically unchanged and there are residual fluctuations in their neighborhoods.

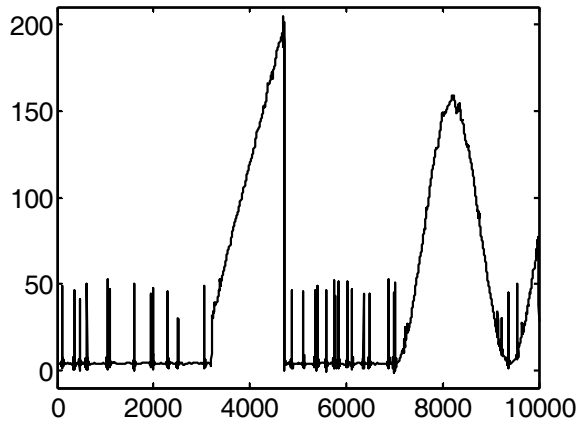

Fig.14. The output signal after the adaptive DCT based filtering of the test signal in Fig. 3

The output signal of the two-stage procedure for which the median filter ($N_{med}=15$) has been used at the second stage is presented in Fig. 15. The impulsive noise is removed and the residual fluctuations are suppressed. This leads to sufficient reduction of σ_{out}^2 (it is equal to 1.52 for the signal in Fig. 15) and P_{exc} (is equal to 0.026). Relative errors also decrease (see the plot in Fig. 16). They are smaller than the threshold 0.2 for the majority of the samples.

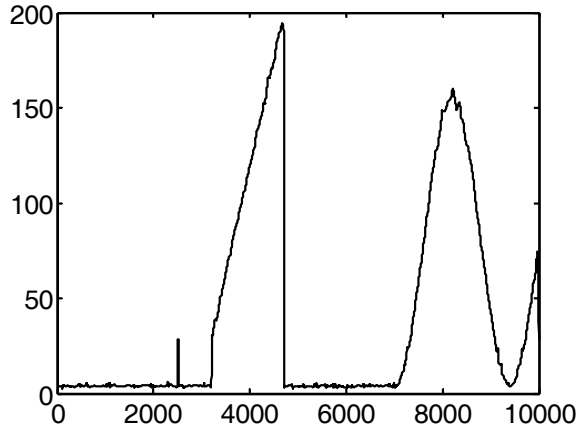

Fig. 15. The output signal for the two-stage filtering

Therefore, the proposed two-stage filtering procedure provides impulsive noise removal, suppression of the

Poisson noise and quite good preservation of the sharp transitions and other important features. The obtained values of σ^2_{out} are smaller that for the method in [3].

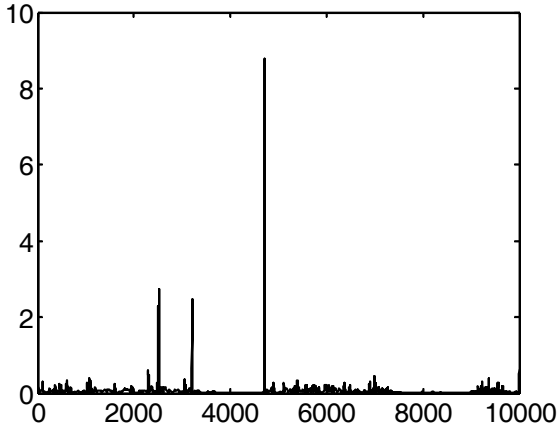

Fig. 16. $\{\Delta S(i)\}$ for the output signal in Fig. 15

Finally, Fig. 17 (grey color) presents the initial real life signal, the same as in Fig. 1, and the output of the DCT based filter that uses $\hat{I}_{bl}^{med}$ (black solid line). The noise is well suppressed, the details are preserved, and there are no effects that have been observed for the median filter output (see Introduction).

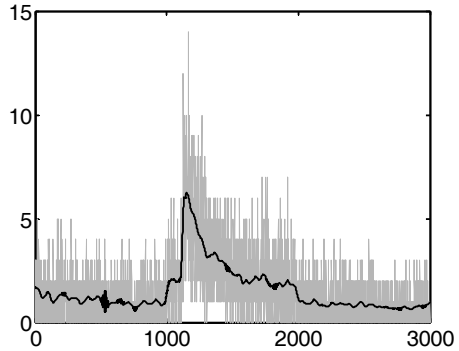

Fig. 17. Initial real life signal (the same as in Fig. 1) and the output of the DCT based filter that uses $\hat{I}_{bl}^{med}$

6. CONCLUSIONS

Two ways of applying the DCT based filtering for the removal of the Poisson noise have been considered. It is demonstrated that the procedure $H(.) \to F(.) \to H^{-1}(.)$ does not provide any benefits in comparison to the adaptive DCT based denosing for which the threshold for each block is set individually using the estimate $\hat{I}_{bl}^{med}$. If the impulsive noise is present, then it is possible to exploit the two stage procedure for which the median filter is applied sequentially to the adaptive DCT based filter output.

ACKNOWLEDGMENTS

This work was supported by the Academy of Finland Project no. 213462 (Finnish Centre of Excellence program 2006-2011).

REFERENCES

[1] Minerskjold M., Sensors, Signals and Systems for Electromagnetic Radiation Experiments in Physics, Ph.D. Thesis, Royal Institute of Technology, Stockholm, Sweden, 1998, 171 p.

[2] Brennan S.M., Mielke A.M., Torney D.C., Maccabe A.B., Radiation Detection with Distributed Sensor Networks, IEEE Computer, Vol. 37, No 8, 2004, 8 p.

[3] Lukin V.V., Peltonen S., Yeltsov P.Ye., Abramov S.K., Besedin A.N., Astola J.T., Removal of Poisson and Impulsive Noise in 1-D Signals by Non-adaptive and Adaptine Nonlinear Filters, Proceedings of NSIP, Bucharest, Romania, Sept. 2007, pp. 110-115.

[4] van Kempen G.M.P., van Vliet L.J., Verveer P.J., van der Voort H.T.M., A Quantitative Comparison of Image Restoration Methods for Confocal Microscopy, Journal of Microscopy, 1997, Vol. 185, pp. 354-365.

[5] Aach T., Kunz D., Multiscale Linear/Median Hybrid Filters for Noise Reduction in Low Doze X-Ray Images, Proceedings of ICIP, 1997, Vol. 2, pp. 358-361.

[6] Hannequin P.P., Mas J.F., Application of iterative and non-stationary smoothing filters for statistical noise reduction in nuclear medicine, Nuclear Medicine Communications, Vol. 19 (9), 1998, pp. 875-885.

[7] Foi A., Alenius S., Trimeche M., Katkovnik V., Egiazarian K.A., Spatially Adaptive Poissonian Image Deblurring, Proceedings of ICIP, 2005, Vol. 2, pp. 925-928.

[8] Yeltsov P., Besedin A., Peltonen S., Lukin V., Statistical Characteristics of Nonlinear Filter Outputs for Poisson Distributed Processes, Proceedings of the 7-th All-Ukrainian Conference on Signal/Image Processing and Pattern Recognition, Kiev, Ukraine, 2004, pp. 69-72.

[9] Anscombe F.J., The transformation of Poisson, binomial and negative binomial data, Biometrica, Vol. 35, 1948, pp. 246-254.

[10] Öktem R., Egiazarian K., Lukin V.V., Ponomarenko N.N., Tsymbal O.V., Locally adaptive DCT filtering for signal-dependent noise removal, EURASIP Journal on Advances in Signal Processing, Vol. 2007, Article ID 42472 (open access paper), 10 pages.

[11] Cheng J.H., Liang Z., Li J., Ye J., Harrington D., Inclusion of a priori information in frequency space for quantitative SPECT imaging, Conference Record of IEEE NSS-MIC, 1996, Vol. 3, pp. 1648 – 1652.

[12] Öktem R., Transform Domain Algorithms for Image Compression and Denoising: Thesis for the degree of Doctor of Technology: Tampere University of Technology (Tampere, Finland), 2000, 142 p.

[13] Donoho D.L., Johnstone I.M., Adapting to unknown smoothness via wavelet shrinkage, JASA, 1995, V. 90, pp. 1200-1224.

[14] Lukin V., Chemerovsky V., Melnik V., Peltonen S., Kuosmanen P., Iterative Procedures for Nonlinear Filtering of Images, Proceedings of the IEEE-EURASIP Workshop on Nonlinear Signal and Image Processing, June 1999, Antalya, Turkey, V.1, pp. 432-436.